Factors Influencing Redox Thermodynamics and Electron Self-Exchange for the $[Fe_4S_4]$ Cluster in *Chromatium vinosum* High Potential Iron Protein: The Role of Core Aromatic Residues in Defining Cluster Redox Chemistry†

Aileen Soriano, Dawei Li, Shumin Bian, Anshu Agarwal, and J. A. Cowan*,‡

Evans Laboratory of Chemistry, The Ohio State University, 100 West 18th Avenue, Columbus, Ohio 43210

Received April 23, 1996; Revised Manuscript Received July 16, 1996⊗

ABSTRACT: The roles of aromatic core residues in regulating the reduction potential, the enthalpy and entropy of reduction, and the self-exchange rate constants for electron-transfer reactions for the prosthetic $[Fe_4S_4]^{3+/2+}$ cluster of *Chromatium vinosum* high potential iron protein (HiPIP) have been addressed by a combination of site-directed mutagenesis, high field NMR (EXSY) experiments, and variable temperature spectrochemical redox titration measurements. Minimal changes are observed following nonconservative mutation of residues Tyr19, Phe48, and Phe66. Apparently these hydrophobic residues play only a minor role in defining the electronic properties of the cluster. These data support a model, first defined from results obtained on Tyr19 mutant HiPIP's [Agarwal, A., Li, D., & Cowan, J. A. (1995) *Proc. Natl. Acad. Sci. U.S.A. 92*, 9440−9444], in which the aromatic core restricts solvent accessibility and thereby stabilizes the oxidized $[Fe_4S_4]^{3+}$ cluster.

Identification of critical factors that define the reduction potentials and electron-transfer chemistry of metalloredox proteins is highly pertinent to understanding their evolutionary design and physiological role. Evaluation and rank ordering of the relative importance of the many possible factors that define the reduction potential and electron-transfer pathways is a focus of current research activity in many laboratories and encompasses both synthetic modeling and protein biochemistry (Agarwal et al., 1993, 1995; Asso et al., 1995; Babini et al., 1996; Bertini et al., 1993; Coucouvanis et al., 1987; Demadis & Coucouvanis, 1995; Holm, 1992; Heering et al., 1995; Luchinat et al., 1994; Shen et al., 1993, 1994; Zhou & Holm, 1995). The pertinent variables include solvent exposure, hydrophobic effects, hydrogen bonding, electric fields from backbone amide dipoles, and bonding contacts mediated by π-complexation. The ability of nature to tune the redox chemistry of biological redox cofactors is well illustrated by the *c*-type cytochromes (−400 to +400 mV) and $[Fe_4S_4]$-cluster proteins (−400 to +450 mV). Bertrand and co-workers (1995) have published an insightful summary of the former and also have evaluated the temperature dependence of low potential clusters in ferredoxins I and II from the sulfate reducing bacterium *Desulfovibrio vulgaris* Miyazaki (Asso et al., 1995). In this paper our attention is focused on the family of high potential $[Fe_4S_4]$ proteins, using *Chromatium vinosum* HiPIP as a vehicle for detailed structure−function studies. It is found that even within the HiPIP family the redox potentials are tuned over a large range, from +50 to +450 mV (Mizrahi et al., 1980). Most high potential iron proteins have been isolated from purple photosynthetic bacteria and vary in size from 6 to 10 kDa. Structures have been determined in the crystalline and/or solution states for HiPIP's from *Chromatium vinosum*, *Ectothiorhodospira halophila I*, *Ectothiorhodospira vacuolata II*, and *Rhodocyclus tenuis* (Breiter et al., 1991; Rayment et al., 1992; Benning et al., 1994; Bertini et al., 1995; Banci et al., 1995; Carter, 1977). The availability of high-resolution structural data facilitates a detailed analysis of cluster chemistry through a site-directed mutagenesis approach (Agarwal et al., 1993).

In recent work we have investigated site-directed mutants of Tyr19 (Agarwal et al., 1995, 1996; Li et al., 1996; Lui & Cowan, 1994), a residue that lies in the hydrophobic cluster-binding pocket and forms a close interaction with the cluster (Figure 1). These studies provided information on the dynamics and bonding interactions of this residue with the cluster and suggested a novel functional role. Kinetic studies of cluster stability and multinuclear NMR methods support a model where Tyr19 serves to maintain a hydrophobic barrier for exclusion of water from the cluster cavity (Agarwal et al., 1995, 1996b; Li et al., 1996). Solvent accessibility results in facile oxidation of the cluster by atmospheric oxygen, with subsequent rapid hydrolysis of the $[Fe_4S_4]^{3+}$ core. In some instances a $[Fe_3S_4]^{+}$ cluster has been identified as an intermediate on the degradation pathway (Agarwal et al., 1996; Bian et al., manuscript submitted). All of these observations are fully consistent with experimental results obtained with model synthetic clusters (Blonk et al., 1991; Roth & Jordanov, 1992). Here we extend these mutational studies to other conserved aromatic residues in the hydrophobic pocket and address how these residues (Tyr19, Phe48, and Phe66; illustrated in Figure 1) influence critical electronic properties of the cluster. The influence of nonconservative mutations on the reduction potentials, enthalpies, and entropies is investigated. The number and orientations of hydrophobic residues that surround the cluster, the extent of solvent accessibility, and the influence of the protein-derived electrostatic field have been cited as critical factors in the control of cluster reduction potentials (E_m's) (Langen et al., 1992; Jensen et al., 1994). Cluster solvation, the proximity of aromatic residues, and hydrogen bonding have been cited in recent published work (Heering et al.,

† Supported in part by NSF Grant Number CHE-8921468.

‡ J.A.C. is currently a Camille Dreyfus Teacher-Scholar (1994−1999) and a National Science Foundation Young Investigator (1992−1997).

⊗ Abstract published in *Advance ACS Abstracts,* September 1, 1996.

S0006-2960(96)00974-9 CCC: $12.00

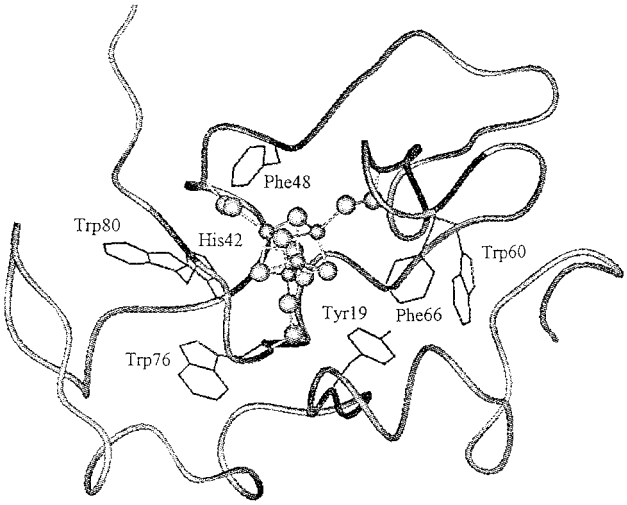

FIGURE 1: Backbone structure of *C. vinosum* HiPIP showing the placement of the key aromatic side chains that form a hydrophobic pocket for the $[Fe_4S_4]$ cluster.

1995) as key factors in discriminating the potentials of various HiPIP's, although the latter has been effectively negated by Rayment et al. (1991) where it has been demonstrated by comparison of crystallographically defined HiPIP's that there is no correlation between hydrogen bonding and E_m. While many hypotheses have been made concerning the factors that control cluster redox properties, it is only since the availability of expression systems, which allow analysis by site-directed mutagenesis, that these ideas have been open to experimental testing. In fact, recent experiments from our laboratory on Tyr19 mutants have emphasized that most of the factors previously speculated to control cluster chemistry actually play a negligible role in defining the reduction potential of the $[Fe_4S_4]$ center (Agarwal et al., 1995; Li et al., 1996). This important conclusion is further reinforced by the results reported in this paper for Tyr19, Phe66, and Phe48 mutants. Surface charge may play a minor role in defining the midpoint potential (E_m) (Luchinat et al., 1994); however, the ability to delocalize charge over amino acid residues and the polarity of the cluster environment appears to be of lesser importance. These issues are of general relevance for understanding the mechanisms employed by proteins for modulating the chemistry of protein-bound redox cofactors. In a related series of experiments, we have investigated, and describe herein, the role of these residues in mediating electron transfer by measuring self-exchange rate constants for representative mutants at each residue site. On the basis of crystallographic results, Carter et al. (1977) have suggested that Tyr19 is a critical residue for mediating electron transfer, while Bertini et al. (1993) have proposed Phe48 as a mediator of electron transfer in the self-exchange reaction of the HiPIP from *E. vacuolata*. In early studies of oxidation−reduction chemistry of HiPIP with nonphysiological reactants, Mizrahi and co-workers (1980) proposed several charge-relay pathways involving Phe48, Phe66, and Trp76 residues. In fact, all of these aromatic residues are widely conserved in the HiPIP family. The studies reported herein form a critical appraisal of the functional role of core Tyr and Phe residues in defining the thermodynamic parameters for cluster redox chemistry and in mediating electron transfer.

MATERIALS AND METHODS

Cell Culture and Protein Purification. Recombinant native (rec-nat) and mutant HiPIP was isolated from an *Escherichia coli* host following expression from a pET-21d-(+) expression vector, as described previously (Agarwal et al., 1993, 1995).

Measurement of Reduction Potentials. Protein reduction potentials were determined by a spectrochemical titration method (Figure 2) (Dutton, 1978). To a quartz cuvette were added 1 μL of a protein stock solution, 100 μL of $Fe(CN)_4^{2-}$ [100 mM stock], and 800 μL of 50 mM potassium phosphate buffer (pH 7.0). Optical spectra were measured on a Hewlett-Packard 84522A spectrophotometer (run by software from On-Line-Instrument Systems). The solution absorbance at 500 nm was typically ca 0.1, which was then equilibrated for at least 15 min at the desired temperature in an optical heat block. Neither $Fe(CN)_4^{2-}$ nor $Fe(CN)_6^{3-}$ absorb significantly at 500 nm, even at very high concentration. After measuring the absorbance of the solution, it was then titrated with 1 μL increments of $Fe(CN)_6^{3-}$ (200 mM stock solution) with subsequent reading of the absorbance at 500 nm after each addition of oxidant. After addition of at least 15 increments of oxidant, 10 μL increments of $Fe(CN)_6^{3-}$ were added until the fully oxidized form of the protein was reached, when no further change in absorbance was noted at 500 nm. The solution potentials were determined after completion of the experiment in order to minimize the time available for protein degradation. Volume changes after each addition were corrected for and the relative concentrations of oxidized and reduced protein were estimated from the limiting absorbance for fully reduced (A_{red}) and fully oxidized (A_{ox}) HiPIP and published extinction coefficients (Bartsch, 1978). The solution potential (E_S) was calculated from the Nernst equation and the known [ferricyanide]/[ferrocyanide] ratio. The influence of ionic strength, pH, and temperature on the ferro-/ferricyanide couple were accounted for according to the literature (O'Reilly, 1973). The midpoint reduction potential (E_m) for the protein was determined from a Nernst plot of the solution potential (E_s) and the absorbance readings using the equation $E_S = E_m + (RT/nF)\ \ln[(A_{red} - A_{obs})/(A_{obs} - A_{ox})]$ (Dutton, 1978), where all other symbols have their usual meanings.

An isothermal configuration was used for variable temperature electrochemical experiments. The temperature of the reduction potential for the ferri/ferrocyanide redox couple at pH 7.0 in 50 mM potassium phosphate was estimated using the equation $E_{T,Fe(III)/Fe(II)} = 0.4182 - \Delta T(0.00252$ V/°C), where $\Delta T = T - 25$ °C and E_m at 25 °C is 0.4182 V (O'Reilly, 1973).

NMR Measurements. ^{1}H NMR spectra were acquired at 500.13 MHz on a BRUKER AM500 spectrometer equipped with ASPECT 3000 data station and using a spectral width that was sufficient to cover both the paramagnetic and diamagnetic regions. Protein samples were at least 3−4 mM in 50 mM potassium phosphate/D_2O (pH 6.4). All experiments were carried out at 15 °C to minimize the autoreduction of oxidized protein. Each sample was titrated with 1 μL aliquots of 500 mM $Fe(CN)_6^{3-}$ until an approximately 1:1 ratio of oxidized and reduced protein was reached

(monitored by comparing the integral of reduced and oxidized hyperfine-shifted peaks in the 1D ^{1}H NMR spectrum). In the case of Tyr19Leu, the sample was thoroughly deaerated by argon purging before addition of oxidant. The sample was kept under an inert atmosphere of argon during data acquisition. Figure 3 shows two-dimensional exchange spectra (EXSY) that were recorded in a phase-sensitive mode with the standard phase-sensitive NOESY pulse sequence and incorporation of an initial WEFT sequence ($180-\tau-90$) to suppress the residual water signal (Inubushi & Becker, 1983). Data were collected over a 25 kHz bandwidth with 256 t_1 blocks and 2048 t_2 points with a mixing time (τ) between 3.5 and 7.5 ms as defined by eq 5 in the text. The data were then processed using 90°-sine-bell-squared apodization over 200 (or 128) t_1 points and 2048 t_2 points and zero-filled to 2048 × 2048 prior to Fourier transformation. One-dimensional spectra of each sample were taken before and after 2D data acquisition to double check the concentration of oxidized and reduced protein. Parameters for specific experiments are described in the figure legends.

Determination of self-exchange rates by 2D EXSY. The use of 2D NMR for kinetic studies was first proposed by Jeener et al. (1979). The main feature of a quantitative 2D EXSY experiment is the relationship between the intensity of a cross-peak and the rate constants defining the chemical exchange. Based on the work of Macura and Ernst (1980), the integrated intensities of the two-dimensional absorption peak can be related to chemical exchange rate constants through a rate (or relaxation) matrix **R**, where the off-diagonal elements are $R_{ij} = -k_{ji}$, the diagonal elements are $R_{ii} = T_{1,i}^{-1} + \sum k_{il}$, and $T_{1,i}$ is the spin−lattice relaxation time of nuclei in site i in the absence of chemical exchange. The rate matrix **R** can be solved to obtain the rate constants for chemical exchange (Perrin, et al., 1984, 1990). The cross-peak intensities can be measured from the volume integral under the cross-peaks if the spectra were obtained in the phase-sensitive mode.

For a self-exchange reaction (1), the second-order rate

$$\mathrm{ox}_2 + \mathrm{red}_1 \underset{k_{-2}}{\overset{k_2}{\rightleftharpoons}} \mathrm{red}_2 + \mathrm{ox}_1 \qquad (1)$$

$$\mathrm{ox(A)} \underset{k_r}{\overset{k_f}{\rightleftharpoons}} \mathrm{red(B)} \qquad (2)$$

constants k_2 and k_{-2} can be estimated by assuming a pseudo-first-order reaction (2), where the forward rate constant $k_f = k_2[\mathrm{red}_1]$, and the reverse rate constant $k_r = k_{-2}[\mathrm{ox}_1]$. The first-order rate constants k_f and k_r are estimated from the experiment, and k_2 and k_{-2} are evaluated from the variation of k_f and k_r with the concentration of redox species.

RESULTS

Characterization and Stability of Mutant Proteins. Isolation, purification, NMR characterization, and stability studies of the mutant proteins used in these studies have been previously described (Agarwal et al., 1993, 1995; Li et al., 1996; Soriano & Cowan, 1996; Bian et al., manuscript submitted). Most mutants, with the exception of Tyr19Phe and Trp, and Phe66Tyr show considerable instability in the oxidized state. This instability may be manifest by either solvolytic cluster degradation, or by an autoreduction pathway that results from the release of reducing equivalents (Fe^{2+} and S^{2-}) by cluster degradation in a portion of the sample (Agarwal et al., 1995, 1996; Soriano & Cowan, 1996; Bian et al., manuscript submitted). Solvent access to the cluster pocket has previously been demonstrated by ^{1}H−^{15}N HMQC experiments (Li et al., 1996; Bian et al., manuscript submitted) and is most pronounced in the case of Tyr19 mutants with polar sidechain replacements.

Temperature and pH Dependence of Reduction Potentials. The net entropy change for the complete cell reaction (referenced to NHE) is given by $\Delta S°_{\mathrm{cell}} = \Delta S°_{\mathrm{rc}} + (nS°_{\mathrm{H^+}} - (1/2)nS°_{\mathrm{H_2}})$, where the $S°$ terms represent partial molal entropies. The entropy difference due to the reference electrode may be separated from that due to the redox couple of interest by use of the third law of thermodynamics, and so the overall cell reaction entropy $\Delta S°_{\mathrm{cell}}$ for a one-electron redox reaction can be written in the form of eq 3, when taking 31.2 eu for the partial molal entropy of H_2, and Latimer's

$$\Delta S°_{\mathrm{cell}} = \Delta S°_{\mathrm{rc}} - 15.6 \text{ eu} \qquad (3)$$

convention of zero for $S°_{\mathrm{H^+}}$. Thus the entropy change for the overall cell reaction $\Delta S°_{\mathrm{cell}}$ (determined from isothermal experiments) is equal to the reaction entropy $\Delta S°_{\mathrm{rc}}$ (determined from nonisothermal experiment) after subtraction of 15.6 eu. Weaver and co-workers have noted that the use of nonisothermal cells avoids certain problems associated with the reference electrode for an isothermal cell configuration (Yee et al., 1979). Previously we have demonstrated the use of nonisothermal direct square-wave voltammetric methods for measurement of metalloprotein reduction potentials (Lui & Cowan, 1994); however, this method was not generally applicable to all of the mutants described in this work as a result of stability/degradation problems. Accordingly, for these studies an isothermal arrangement was employed, although the temperature and ionic strength dependence of the reference electrode was accounted for (O'Reilly, 1973). The reduction potential and thermodynamic parameters of rec-nat and mutant HiPIP's were determined by standard spectrochemical titration and variable temperature methods (Dutton, 1978), using a ferro/ferricyanide couple to poise the solution potential and serve as a mediator. The solution absorbance was monitored at 500 nm, where neither ferro- nor ferricyanide absorb. The value of ΔS for the overall cell reaction was determined using the standard thermodynamic relationship (eq 4)

$$-nFE_{\mathrm{m}} = \Delta H - T\Delta S \qquad (4)$$

from the slope of an E_{m} versus T plot, while the enthalpy change ΔH was determined from the intercept (Figure 2B).

Since the redox mediator and other solution conditions are the same for each protein under investigation, a direct comparison of experimental results affords meaningful interpretations in terms of the observed trends. Table 1 demonstrates that the cluster potentials of mutants, measured at 298 K in 50 mM phosphate (pH 7), are generally found to increase by less than 30 mV, with the exception of the Cys77Ser mutant reported in earlier work where a decrease in potential of 30 mV is observed as a result of the replacement of sulfur by an oxygen ligand atom (Agarwal et al., 1996). This modest change in potential was also reflected in the thermodynamic parameters. With the exception again of the Cys77Ser mutant, where a directly

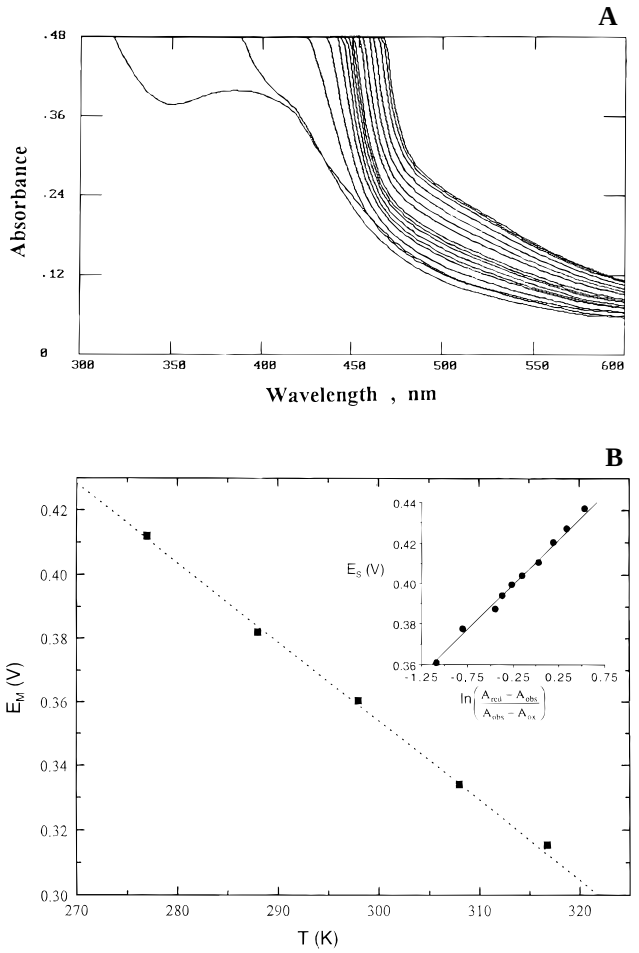

FIGURE 2: Spectroelectrochemical titration experiment on Phe48His in 50 mM potassium phosphate, pH 7, at 4 °C. (A) Overlapping spectra showing the increasing absorbance with increasing [ferricyanide] at 4 °C. (B) Plot of E_m versus T (K) for Phe48His. The inset shows an example of plot of E_S versus log $[(A_{red} - A)/(A - A_{ox})]$ for the data shown in panel A.

Table 1: Reduction Potentials (25 °C) and Thermodynamic Parameters for rec-nat HiPIP and Mutants[a]

	E_m (mV)	ΔH (kcal mol^{-1})	ΔS (cal K^{-1} mol^{-1})
native	345	−32.2	−81.4
Cys77Ser	315	−19.4	−40.7
Tyr19Trp	372	−30.4	−73.2
Tyr19Leu	370	−25.0	−55.4
Tyr19His	348	−26.4	−61.8
Phe66Tyr	356	−25.0	−56.2
Phe66Cys	361	−27.1	−63.1
Phe66Ser	368	−25.4	−56.6
Phe66Asn	392	−25.1	−54.0
Phe48His	360	−25.3	−57.1
Phe48Arg	368	−26.0	−59.3

[a] The standard reduction potential E_m values are averages of three measurements for each protein. Standard deviations are as follows: E_m, ±7 mV; ΔH, ±2 kcal mol^{-1}; ΔS, ±5 cal K^{-1} mol^{-1}.

coordinating ligand atom has been replaced, the data in Table 1 show that ΔH was typically found to be around 5−7 kcal mol^{-1} less negative than the result for rec-nat. A slightly broader range of change is observed for ΔS, which shows a less negative entropy in the range of 8−27 cal K^{-1} mol^{-1} (or 0.8−8 kcal mol^{-1} at 298 K). It is noteworthy that those mutants displaying the largest change in ΔH and ΔS also exhibit the most noticeable changes in solvent accessibility. The Cys77Ser mutant was the sole exception to the observed trends with ΔH and ΔS values reported as −19.4 and −40.7 cal K^{-1} mol^{-1}, respectively (Agarwal et al., 1996). Previously Heering et al. (1995) have reported ΔH and ΔS values of −80.0 kJ mol^{-1} (−19.1 kcal mol^{-1}) and −158.2 J K^{-1} mol^{-1} (−37.8 cal K^{-1} mol^{-1}) for native *C. vinosum* HiPIP, which are similar to our data after accounting for the distinct solution conditions.

Using the spectroelectrochemical method, we were able to measure potentials at temperatures higher than 26 °C for rec-nat and Phe48 mutants. Figure 2B shows no evidence of the break observed by Heering et al. (1995) for *R. gelatinosus* HiPIP, which was ascribed to loss of an hydrogen bond in the oxidized state, and suggested for other HiPIP's including the *C. vinosum* protein.

The pH dependence of E_m shown by the Phe48His and Arg mutants were similar to that of rec-nat (Heering et al., 1995), indicating that an ionizable residue at this site has little electrostatic influence on the cluster potential. This is consistent with the absence of a significant change in E_m for these mutants, relative to rec-nat, and indicates that the small shift most likely arises from minor structural perturbations rather than electrostatic factors.

^{1}H NMR and Self-Exchange Electron-Transfer Rates for rec-Native and Mutant HiPIP. Under our experimental conditions, only three pairs of signals were found to show cross-peaks in the EXSY spectrum of partially oxidized rec-nat HiPIP (Figure 3A). They were from Cys77 β-CH1, Cys77 β-CH2, and Cys 43 β-CH1 protons in the reduced and oxidized forms. The experiments were performed using different mixing times (5, 6, 7.5, 10, and 12.5 ms), and the cross-peaks patterns were found to be similar. The calculated pseudo-first-order rate constants for forward and reverse reactions, defined by eq 2, are listed in Table 2. The second-order rate constants were obtained from the reaction defined by eq 1. The rate constants calculated for a variety of mixing times (5.0, 6.0, and 7.5 ms) were found to be similar and within the range of experimental error. The experimental errors come from two sources. First, the uncertainty in the intensity measurement, and second, the uncertainty in the ratio or absolute values of the concentrations. Those rate constants calculated for mixing times of 10.0 and 12.5 ms are relatively too large or too small, respectively. The optimum value for the mixing time was estimated by use of eq 5 (Perrin & Dwyor, 1990).

$$\tau_{m,opt} \sim 1/({T_1}^{-1} + k_f + k_r) \quad (5)$$

If we take an average T_1 value (15 ms for Cys77 β-CH1) and the pseudo-first-order rate constants k_f and k_r, then the optimum mixing time was estimated as 5.9 ms by use of eq 5. If we average the pseudo-first-order rate constants obtained at 303 K from mixing times of 5.0, 6.0, and 7.5 ms, the average lifetimes of oxidized ($1/k_f$) and reduced ($1/k_r$) forms were calculated as 32.1 and 41.5 ms, respectively. Comparing these lifetimes with the T_1 values of the paramagnetically shifted protons (Cowan & Sola, 1990; Banci et al., 1993), only the Cys77 β-CH1, Cys77 β-CH2, and Cys 43 β-CH1 protons have sufficiently long spin−lattice relaxation times in both oxidized (8, 29, and 21 ms) and reduced (15, 22, and 9 ms) states to permit the detection of magnetization transfer that accompanies electron transfer. Accordingly, the average self-exchange rate constant of rec-nat HiPIP from three mixing times: 5.0, 6.0 and 7.5 ms, is

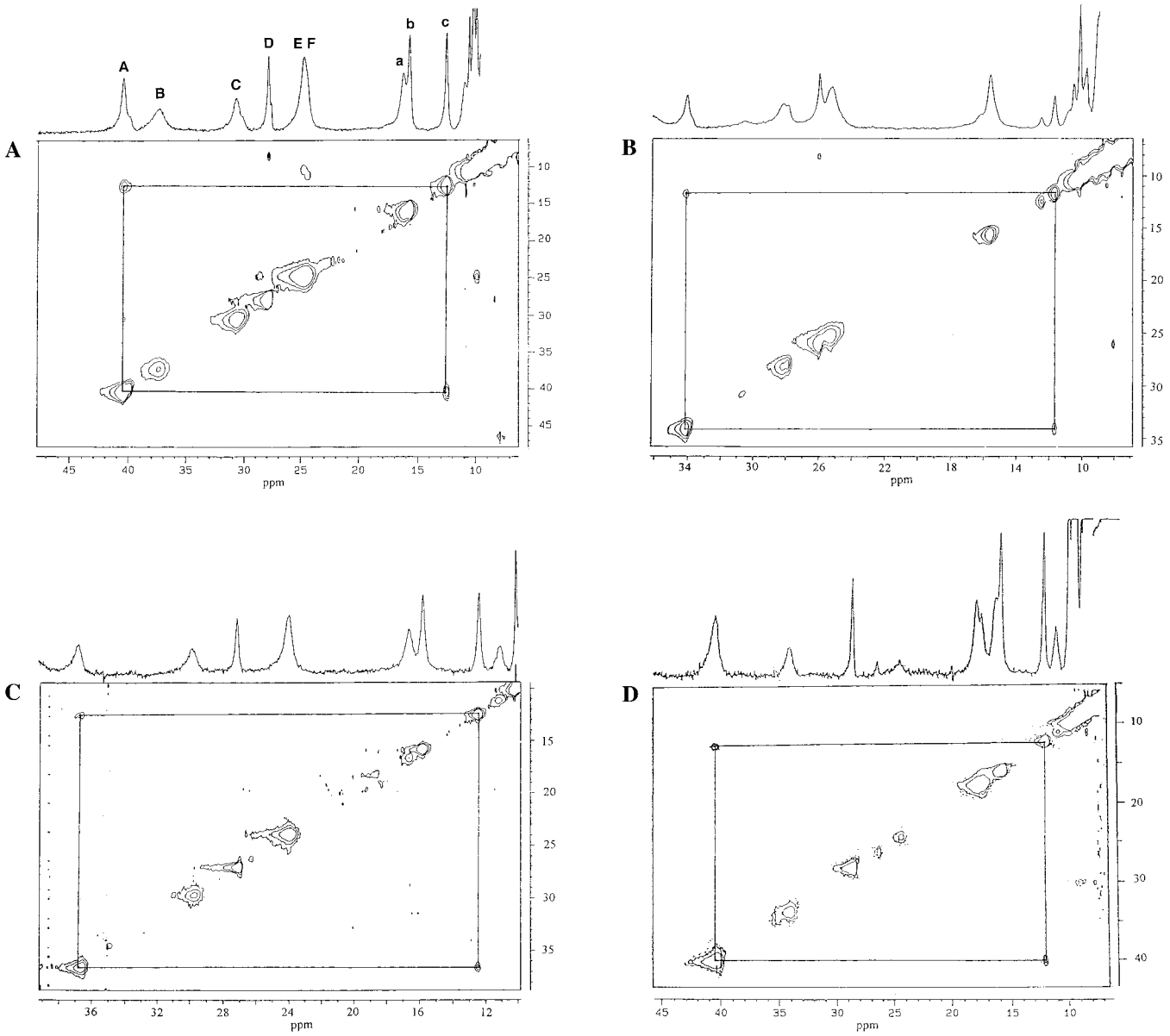

FIGURE 3: 500 MHz ^{1}H NMR EXSY spectra of a redox mixture of the rec-nat and mutant HiPIP's at 288 K: (A) rec-nat; (B) Tyr19Leu; (C) Phe48His; (D) Phe48Arg. Peak assignments for rec-nat are indicated as follows: oxidized, a = Cys77Hβ1, B = Cys63Hβ1, C = Cys77Hβ2, D = Cys77Hα, E = Cys46Hβ1, F = Cys46Hβ2; reduced, a = Cys43Hβ2, b = Cys63Hβ2, c = Cys77Hβ1. Assignments for mutant proteins have been detailed elsewhere (Bian et al., 1996). Electron self-exchange rate constants (k_2, k_{-2}) listed in Table 3 were obtained from well-resolved redox pairs (connected by solid lines). Other experimental details are noted in the legend to Table 3.

Table 2: Second-Order (k_2 and $k_{-2} \times 10^{-3}$ M^{-1} s^{-1})[a] Rate Constants for Electron Self-Exchange Obtained from ^{1}H 2D EXSY Experiments of rec-nat HiPIP with a Variety of Mixing Times (τ_m, ms) and Temperatures (T °C)[b]

τ_m (ms)	k_2 (M^{-1} s^{-1})	k_{-2} (M^{-1} s^{-1})	k (M^{-1} s^{-1})[c]	T (°C)	k_2 (M^{-1} s^{-1})	k_{-2} (M^{-1} s^{-1})	k (M^{-1} s^{-1})[c]
5.0	28.6	24.2	26.4	10	17.0	16.1	16.6
6.0	31.2	26.0	28.6	15	18.5	18.5	18.5
7.5	31.4	30.5	31.0	20	22.4	22.4	22.4
10.0	46.3	46.4	46.4	25	23.0	23.1	23.1
12.5	18.5	18.5	18.5	30	31.2	26.0	28.6
				35	31.8	31.9	31.9

[a] The concentration of the purely reduced form is 2.6 mM. The second-order rate constants k_2 and k_{-2} were calculated with the concentration ratio of [ox]/[red] $\cong$ 1.21 and at 303 K. All rate constants have been multiplied by a constant of 10^{-3}. Errors in these measured rate constants (k) are on the order of ±20%. [b] The mixing time is 6 ms for the variable temperature experiments. [c] $k = (k_2 + k_{-2})/2$.

31.2×10^3 M^{-1} s^{-1} for forward, and 26.9×10^3 M^{-1} s^{-1} for reverse electron transfer at 303 K. These values can be considered as equal within experimental error. Likewise, the electron exchange rates determined for a variety of representative mutant proteins are usually within a factor of two of the rate for rec-nat.

Rate measurements were also made at different temperatures (10−35 °C) for rec-nat HiPIP using a mixing time of 6.0 ms. The pseudo-first-order, second-order, and the average of second-order rate constants, $k = (k_2 + k_{-2})/2$, are also listed in Table 2. By use of the Eyring equation, $k = (\boldsymbol{k}T/h) \exp(-\Delta G^*/RT)$, where the constants have their

usual meanings, a plot of ln k versus $1/T$ from the data in Table 2 yielded an activation energy ΔH^* of 4.0 kcal mol^{-1} and a ΔS^* of -39 cal K^{-1} mol^{-1} for the rec-nat protein.

DISCUSSION

General Comparison of Thermodynamic Parameters. Since the enthalpies and entropies of metalloprotein electron-transfer processes are influenced by changes in protein conformation and solvation, as well as by other structural and medium effects (Taniguchi et al., 1980, 1982a,b), comparison of these parameters over a range of HiPIP's differing by single point mutations can afford considerable insight on the factors underlying the redox chemistry of a metalloprotein. High potential iron proteins are a particularly attractive choice for such a study since several have been structurally characterized by crystallography and solution NMR methods (Breiter et al., 1991; Rayment et al., 1992; Benning et al., 1994; Bertini et al., 1995; Banci et al., 1995; Carter, 1977), while strategies for addressing solvent accessibility and the influence of charge and solvation on cluster potentials have been demonstrated (Agarwal et al., 1995, 1996; Li et al., 1996).

Surprisingly few reports of the temperature dependence of [Fe_4S_4] cluster potentials have appeared in the literature. Heering et al. (1995) have published a report that reviews a large family of HiPIP's. The thermodynamic data conflicted with an earlier study of Taniguchi et al. (1980) but are reasonably consistent with our own measurements when considering the distinct solution conditions and methods employed. With the exception of a small number of *c*-type cytochromes, the enthalpic component is typically found to be negative for the available data on heme proteins and [Fe_4S_4] proteins, reflecting favorable bonding changes upon reduction. For HiPIP's, the ΔH values typically lie within $4-5$ kcal mol^{-1} of each other, which is consistent with their similar E_m's and the importance of the enthalpy term in defining the free energy for reduction. The enthalpy changes are usually more negative for the $[Fe_4S_4]^{3+/2+}$ couple than for the $Fe^{3+/2+}$ heme couple in cytochromes (Bertrand et al., 1995), presumably as a result of favorable interactions between the cluster and the polypeptide, including coordination from four cysteine residues and favorable interactions with aromatic rings.

The values of the entropy change ΔS (at pH 7.0 and 25 °C) are all negative in magnitude (Table 1), in contrast to typical results obtained for transition metal complexes which usually show a positive entropy change for positively charged metal complexes and a negative entropy change for negatively charged metal complexes (Borchardt & Wherland, 1994; Sutin et al., 1980; Yee et al., 1979). Electrostatic charge factors and specific ligand solvation effects appear to dominate the entropy change exhibited by transition metal complexes (Yee et al., 1979). Bulky and hydrophobic ligands (phenanthroline and bipyridine, for example) depress the magnitude of the observed ΔS. In contrast, metalloprotein redox couples tend to show negative entropy changes that do not correlate with protein charge (Taniguchi et al., 1980, 1982a,b; Yee et al., 1979). The negative entropy change is dominated by the structural change of the protein backbone and side chains upon reduction. The entropy changes are significantly more negative relative to other redox proteins, consistent with the apparent rigidity of the HiPIP structure (Taniguchi et al., 1980). The similarity in structure for reduced and oxidized HiPIP's has been demonstrated both by solution NMR studies and crystallography (Carter, 1977; Rayment et al., 1991; Banci et al., 1995; Bertini et al., 1995).

Native HiPIP shows the most negative enthalpy and entropy change. The Cys77Ser mutant has been discussed in detail elsewhere (Agarwal et al., 1996) and will be considered no further here. Of the other mutants, most show enthalpy and entropy changes that are less negative relative to rec-nat, except in the case of certain conservative mutations such as Tyr19Trp (Table 1). The larger changes arise for those mutants where there is enhanced solvent accessibility to the cluster binding pocket. A change in solvent accessibility does not, therefore, result in a substantive change in E_m since the favorable entropy change is offset by a less favorable change in the reaction enthalpy. This is somewhat analogous to the situation observed for cytochromes with positive E_m values as described recently and summarized immediately below.

Implications for Results Obtained from Native and Mutant HiPIP's. Bertrand et al. (1995) have recently presented a detailed account of factors controlling the redox potential of *c*-type and *b*-type cytochromes. As for [Fe_4S_4] proteins, cytochromes span a wide range of reduction potentials (-400 to $+400$ mV). The general conclusion by Bertrand was that the solvent accessibility of the heme propionates was a dominating factor in the control of heme potential for those hemes with a positive E_m. These workers also noted a very strong enthalpy−entropy compensatory relationship between cytochromes that had similar E_m's, but possessed widely varying ΔH and ΔS values.

The results obtained for Phe66, Phe48, and Tyr19 mutants show no such dramatic differences. Not only the E_m's but also the enthalpic and entropic components were found to be similar. Only in the case of a Cys77Ser mutation have significant differences in the thermodynamic parameters been observed, although again the E_m was relatively unperturbed (30 mV lower). In spite of the apparent simplicity of the observations, our results are, in fact, highly significant. On the basis of crystallographic and NMR evidence, the aromatic rings of both Phe66 and Tyr19 display close interactions with the iron−sulfur cluster (Carter, 1977; Rayment et al., 1991). These interactions are removed in the mutant proteins. The similarity in E_m, ΔH, and ΔS values suggests that these interactions serve little role in defining cluster redox chemistry. Another, and perhaps more significant, observation is the absence of any significant change in the redox properties of the cluster with the increasing solvent accessibility that has previously been demonstrated for these mutant proteins (Agarwal et al., 1995; Bian et al., manuscript submitted).

Some useful comparisons can be made with the available literature on model systems, although as for the situation with iron−sulfur proteins there is a paucity of data on systematic studies of solvent effects on E_m, and in particular the available detailed thermodynamic data on redox properties of model [Fe_4S_4] clusters are sparse. The influence of varying solvent dielectric on the reduction potentials has been examined by Blonk et al. (1991) for the cluster series [$Fe_4S_4(SR)_4$]. When R = Ph, a minimal variation in E_m was observed for both the high and low potential couples. For example, in nitrobenzene ($\epsilon = 35.7$) $E_m = -0.33$ V, while

in dichloromethane ($\epsilon = 9.1$) $E_m = -0.32$ V for the high potential couple. Also, when R = ^{t}Bu, $E_m = -0.65$ V in dichloromethane and -0.70 V in *N*,*N*-dimethylformamide ($\epsilon = 37.6$). Similar minimal variations in E_m values were observed for the low potential redox couple. Unfortunately, there is little in the way of systematic data available for the enthalpic and entropic contributions to these potentials. One might expect a range of entropy values that reflect the various dielectric constants and donor numbers of the solvents used. If such variations do exist, then they must be offset by compensatory changes in ΔH. The key observation in these data is, however, the lack of a substantive shift in E_m with solvent. This is consistent with the observations made for the mutant HiPIP's described herein and seems to indicate that the lack of sensitivity of the $[Fe_4S_4]$ cluster potentials to solvent is an effect that is neither limited to, nor a result of, the presence of a protein matrix.

Heering et al. (1995) have argued that HiPIP's may be considered to fall into two classes. One with an E_m independent of the total charge and centered around 336 mV, and one where E_m is dependent on the total charge. After subtraction of the contribution from the overall charge, it was proposed that the remaining part of the potential reflected variations of polarity and solvation in the local cluster environment. However, the results of our studies on mutant proteins indicate no clear role for changes in the polarity of residues neighboring the cluster and provide a clear indication that solvation is not a critical factor. Inasmuch as the electrostatic influence of surface charged residues is likely to be quenched by solvation with a medium (water) of high dielectric constant, trends of potential versus charge and versus absorption maxima must be interpreted with some caution. The results of our mutational studies do not support any significant role in the definition of cluster potential. Rather, as defined in other work from our laboratory, these residues appear to inhibit solvent access to the cluster pocket that can result in hydrolytic degradation of the $[Fe_4S_4]^{3+}$ center.

It has also been argued that stabilization of the reduced state by polar residues leads to a more favorable E_m and a more negative enthalpy change. However, this hypothesis is not supported by the critical experimental tests afforded by our experiments on mutant HiPIP's. Furthermore, in work by Burgess and co-workers (Shen et al., 1993, 1994) on the low potential $[Fe_4S_4]$ ferredoxin centers in *Azotobacter vinelandii* and *Peptococcus aerogenes*, it is found that the E_m's differ by more than 200 mV despite the highly conserved arrangement of residues around the clusters. In these cases mutation of surface charged residues had little effect on E_m, and neither did mutation of two inner hydrophobic residues, one of which resulted in minor structural changes that resulted in perturbed EPR and NMR spectra.

The question remains, then, as to what are the critical factors that define the redox enthalpies and entropies. We have described elsewhere that much of our work on mutant HiPIP's appears to support the model of Jensen et al. (1994) that dipoles from backbone amides are the key factor that define E_m for four-iron ferredoxins. Inasmuch as the electrostatic field from these dipoles will not be greatly perturbed by the mutations described, the entropy and enthalpy terms arising from the cluster, bathed in this field, are essentially defined by the bonding within the cluster and to the cysteines. As stated earlier, notably only in the case of the Cys77Ser mutant was a significant change in ΔH or ΔS observed.

In one of the very few papers addressing the detailed thermodynamics of $[Fe_4S_4]^{2+/+}$ cluster redox reactions in a low potential ferredoxin, Asso et al. (1995) have reported on the EPR and redox characteristics of ferredoxins I and II from *D. vulgaris* Miyazaki. For the $[Fe_4S_4]^{2+/+}$ couple in Fd II, $\Delta H = +2.3$ kcal mol^{-1} ($+9.65$ kJ mol^{-1}) and $\Delta S = -24.6$ cal K^{-1} mol^{-1} (-103 cal K^{-1} mol^{-1}), which demonstrated that the 760 mV difference in potential for these two clusters arises from enthalpic effects. While low potential clusters in Fd's tend to lie closer to the protein surface and are more solvent exposed, our data indicate that this fact does not explain the difference in ΔH terms, and neither does a local variation in side chain identity. Again, the electrostatic field derived from amide dipoles appears to be the most reasonable alternative.

Self-Exchange Rates for Native and Mutant HiPIP. The electron self-exchange transfer rate constants for rec-nat and mutant HiPIP's have been estimated using ^{1}H 2D EXSY methods. Since the mixing time was carefully chosen, the results are relatively dependable (Perrin & Dwyor, 1990). The average electron-transfer rate constants (28.6×10^3 M^{-1} s^{-1} at 303 K) are about 10 times slower than those estimated by 1D NOE methods ($\sim 3 \times 10^5$ M^{-1} s^{-1}) (Bertini, 1993; although these data were collected at pH 5 and a slower rate would be expected for an acidic protein), but a little faster than that evaluated from T_1 measurements of the redox mixture (1.7×10^4 M^{-1} s^{-1}) (Sola et al., 1989). The mixing times used in the experiment were estimated from eq 5, using the exchange rates estimated from ^{1}H NMR data from rec-nat HiPIP, and the total concentration of rec-nat or mutant HiPIP.

Previously, it has been noted that the redox kinetics of *C. vinosum* HiPIP do not depend on the ionic strength of the solvent, although the net charge of the peptide chain is -3 at pH 7.0 (Mizrahi, et al.,1980). Since the exchange of electrons between reduced and oxidized HiPIP molecules requires direct protein−protein contact, it is likely that neutralization of charged residues at the binding interface is required for electrostatic stabilization. An increase in self-exchange rate constants with decreasing pH has previously been observed for *C. vinosum* HiPIP (Mizrahi et al., 1980).

Self-exchange rate constants have been measured for model $[Fe_4S_4]$ clusters. These reactions are bimolecular and outer-sphere with rate constants $k \sim 10^6-10^7$ M^{-1} s^{-1}. In the particular case of the complex $[Fe_4S_4(S\text{-}p\text{-}C_6H_4CH_3)_4]^{2-}$ with a self-exchange rate constant at 298 K of 2.8×10^6 M^{-1} s^{-1} and activation parameters of $\Delta H^* = 3.6$ kcal mol^{-1} and $\Delta S^* = 17$ cal K^{-1} mol^{-1} have been determined (Reynolds et al., 1978). Comparison with data from rec-nat HiPIP ($\Delta H^* \sim 5.1$ kcal mol^{-1}, $\Delta S^* \sim -305$ cal K^{-1} mol^{-1}), which shows a rate constant of 2.3×10^4 M^{-1} s^{-1} at 298 K, demonstrates similar ΔH^* but very distinct ΔS^* values. This trend matches the finding for the ground state thermodynamic parameters in that the entropic term is strongly negative for the protein, a reflection again of the rigid protein structure and the absence of significant bonding and conformational changes required to reach the transition state for the reaction.

Aromatic side chains surrounding the cluster have long been believed to mediate electron transfer reactions, both

Table 3: Second-Order Electron Transfer Rate Constants for Self-Exchange of rec-nat and Mutant HiPIP's

sample	k_2 ($\times 10^{-3}$ M^{-1} s^{-1})	k_{-2} ($\times 10^{-3}$ M^{-1} s^{-1})	k ($\times 10^{-3}$ M^{-1} s^{-1})
rec-nat	13.5	16.1	14.5
Phe48His	9.3	10.8	10.0
Phe48Arg	4.0	5.9	5.0
Phe66Ser	12.2	14.4	13.3
Tyr19Leu	23.0	26.2	24.5

[a] The concentrations of the purely reduced forms were as follows: [rec-nat] = 3.98 mM; [Phe48His] = 3.98 mM; [Phe48Arg] = 3.44 mM; [Phe66Ser] = 3.72 mM; [Tyr19Leu] = 2.72 mM. The second-order rate constants (k_2 and k_{-2}) were calculated according to the following ratios of [ox]/[red] and mixing times: rec-nat, 1.17, 3.5 ms; Phe48His, 0.74, 4 ms; Phe48Arg, 3.44, 3.5 ms; Phe66Ser, 1.26, 3.5 ms; Tyr19Leu, 1.2, 4.0 ms. EXSY data were obtained at 288 K. Errors in these measured rate constants (k) are on the order of ±20%.

self-exchange reactions and electron-transfer with other redox partners. The data summarized in Table 3 suggest otherwise. Relative to rec-nat HiPIP, the exchange rates for the mutant proteins differ by no more than a factor of 2. These observations are also consistent with the pathway approach of Beratan et al. (1992), which tends to emphasize σ-bonding pathways in mediating electron transfer through a protein framework. A critical appraisal of the available experimental data, particularly for mutant proteins, suggests that the role of aromatic core is to prevent solvent access that might compromise the stability of the oxidized cluster (Stout, 1982) rather than to mediate cluster redox potentials or electron-transfer.

The conclusion from these studies is that neither specific aromatic amino acid side chains nor solvent accessibility appear to play a major role in defining the reduction potentials or electron-transfer properties of the cluster in high potential iron proteins. The role of the aromatic core is to maintain a hydrophobic barrier to solvent water and inhibit oxidation and hydrolytic degradation of the cluster (Li et al., 1996; Bian et al., 1996). This role was previously developed for Tyr19 and appears to be more generally applicable.

REFERENCES

Agarwal, A., Li, D., & Cowan, J. A. (1995) *Proc. Natl. Acad. Sci. U.S.A. 92*, 9440−9444.

Agarwal, A., Li, D., & Cowan, J. A. (1996) *J. Am. Chem. Soc. 118*, 927−928.

Agarwal, A., Tan, J., Eren, M., Tevelev, A., Lui, S. M., & Cowan, J. A. (1993) *Biochem. Biophys. Res. Commun. 197*, 1357−1362.

Asso, M., Mbarki, O., Guigliarelli, B., Yagi, T., & Berrand, P. (1995) *Biochem. Biophys. Res. Commun. 211*, 198−204.

Babini, E., Bertini, I., Borsari, M., Capozzi, F., Dikiy, A., Eltis, L. D., & Luchinat, C. (1996) *J. Am. Chem. Soc. 118*, 75.

Banci, L., Bertini, I., Ciurli, S., Ferretti, S., Luchinat, C., & Picioli, M. (1993) *Biochemistry 32*, 9387.

Banci, L., Bertini, I., Dikiy, A., Kastrau, D. H. W., Luchinat, C., & Sompornpisut, P. (1995) *Biochemistry 34*, 206.

Bartsch, R. G. (1978) *Methods Enzymol. 53*, 329−340.

Benning, M. M., Meyer, T. E., Rayment, I., & Holden, H. M. (1994) *Biochemistry 33*, 2476−2483.

Beratan, D. N., Onuchic, J. N., Winkler, J. R., & Gray, H. B. (1992) *Science 258*, 1740−1741.

Bertini, I., Gaudemer, A., Luchinat, C., & Piccioli, M. (1993) *Biochemistry 32*, 12887.

Bertini, I., Dikiy, A., Kastrau, D. H. W., Luchinat, C., & Sompornpisut, P. (1995) *Biochemistry 34*, 9851.

Bertrand, P., Mbarki, O., Asso, M., Blanchard, L., Guerlesquin, F., & Tegoni, M. (1995) *Biochemistry 34*, 11071−11079.

Blonk, H. L., Kievit, O., Roth, E. K. H., Jordanov, J., van der Linden, J. G. M., & Steggerda, J. J. (1991) *Inorg. Chem. 30*, 3231−3234.

Borchardt, D., & Wherland, S. (1984) *Inorg. Chem. 23*, 2537.

Breiter, D. R., Meyer, T. E., Rayment, I., & Holden, H. M. (1991) *J. Biol. Chem. 266*, 18660−18667.

Carter, C. W., Jr. (1977) In *Iron-Sulfur Proteins III* (Lovenberg, W., Ed.) pp 157−204, Academic Press, New York.

Coucouvanis, D., Kanatzidis, M. G., Salifoglou, A., Dunham. W. R., Simopoulos, A., Sams, J. R., Papaefthymiou, V., & Kostikas, A. (1987) *J. Am. Chem. Soc. 109*, 6863.

Demadis, K. D., & Coucouvanis, D. (1995) *Inorg. Chem. 34*, 436.

Dutton, P. L. (1978) *Methods Enzymol. 54*, 411.

Heering, H. A., Bilsink, Y. B. M., Hagen, W. R., & Meyer, T. E. (1995) *Biochemistry 211*, 198−204.

Holm, R. H. (1992) *Adv. Inorg. Chem. 38*, 1.

Inubushi, T., & Becker, E. D. (1983) *J. Magn. Reson. 51*, 128.

Jeener, J., Meier, B. H., Bachmann, P., & Ernst, R. R. (1979) *J. Chem. Phys. 71*, 4546.

Jensen, G. M., Warshel, A., & Stephens, P. J. (1994) *Biochemistry 33*, 10911.

Langen, R., Jensen, G. M., Jacob, U., Stephens, P. J., & Warshel, A. (1992) *J. Biol. Chem. 267*, 25625.

Li, D., Agarwal, A., & Cowan, J. A. (1996) *Inorg. Chem. 35*, 1121−1125.

Luchinat, C., Capozzi, F., Borsari, M., Battistuzzi, G., & Sola, M. (1994) *Biochem. Biophys. Res. Commun. 203*, 436−442.

Lui, S. M., & Cowan, J. A. (1994) *J. Am. Chem. Soc. 116*, 4483.

Macura, S., & Ernst, R. R. (1980) *Mol. Phys. 41*, 95−117.

Mizrahi, I. A., Meyer, T. E., & Cusanovich, M. A. (1980) *Biochemistry 19*, 4727.

O'Reilly, J. E. (1973) *Biochim. Biophys. Acta 292*, 509.

Perrin, C. L., & Dwyer, T.-J. (1990) *Chem Rev. 90*, 935.

Perrin, C. L., Dwyer, T. J., & Baine, P. (1994) *J. Am. Chem. Soc. 116*, 4044−4049.

Rayment, I., Wesenberg, G., Meyer, T. E., Cusanovich, M. A., & Holden, H. M. (1992) *J. Mol. Biol. 228*, 672−686.

Reynolds, J. G., Laskowski, E. J., & Holm, R. H. (1978) *J. Am. Chem. Soc. 100*, 5315−5322.

Roth, E. K. H., & Jordanov, J. (1992) *Inorg. Chem. 31*, 240−243.

Shen, B., Martin, L. L., Butt, J. N., Armstrong, F. A., Stout, C. D., Jensen, G. M., Stephens, P. J., La Mar, G. N., Gorst, C. M., & Burgess, B. K. (1993) *J. Biol. Chem. 268*, 25928.

Shen, B., Jollie, D. R., Stout, C. D., Diller, T. C., Armstrong, F. A., Gorst, C. M., La Mar, G. N., Stephens, P. J., & Burgess, B. K. (1994) *J. Biol. Chem. 269*, 8564.

Sola, M., Cowan, J. A., & Gray, H. B. (1989) *J. Am. Chem. Soc. 111*, 6627.

Soriano, A., & Cowan, J. A. (1996) *Inorg. Chim. Acta* (in press).

Stout, C. D. (1982) in *Metal Ions in Biology* (Spiro, T. G., Ed.) Vol. 4, Chapter 3, John Wiley and Sons, New York.

Sutin, N., Weaver, M. J., & Yee, E. L. (1980) *Inorg. Chem. 19*, 1096.

Taniguchi, V. T., Sailasuta-Scott, N. S., Anson, F. C., & Gray, H. B. (1980) *Pure Appl. Chem. 52*, 2275−2282.

Taniguchi, V. T., Ellis, W. R., Jr., Cammarata, V., Webb, J., Anson, F. C., & Gray, H. B. (1982a) in *Electrochemical and Spectrochemical Studies of Biological Redox Components* (Kadish, K. M., Ed.) p 51, American Chemical Society, Washington D.C.

Taniguchi, V. T., Malmstrom, B. G., Anson, F. C., & Gray, H. B. (1982b) *Proc. Natl. Acad. Sci. U.S.A. 79*, 3387.

Yee, E. L., Cave, R. J., Guyer, K. L., Tyma, P. D., & Weaver, M. J. (1979) *J. Am. Chem. Soc. 101*, 1131.

Zhou, J., & Holm, R. H. (1995) *J. Am. Chem. Soc. 117*, 11353−11354.

BI960974X